Journal of Hydrology 519 (2014) 94–105

Contents lists available at ScienceDirect

Journal of Hydrology

journal homepage: www.elsevier.com/locate/jhydrol

Characterisation of hyporheic exchange in a losing stream using radon-222

Sarah A. Bourke [a,b,*], Peter G. Cook [a,c], Margaret Shanafield [a], Shawan Dogramaci [d], Jordan F. Clark [e]

[a] National Centre for Groundwater Research and Training (NCGRT), School of the Environment Flinders University, GPO Box 2100, SA, Australia
[b] Commonwealth Scientific and Industrial Research Organization (CSIRO), Division of Land and Water, Floreat, Private Bag 5, Wembley 6913, WA, Australia
[c] Commonwealth Scientific and Industrial Research Organization (CSIRO), Division of Land and Water, Glen Osmond, Adelaide, SA 5064, Australia
[d] Rio Tinto Iron Ore, 162-168 St Georges Tce, Perth, WA 6000, Australia
[e] Department of Earth Science, University of California, Santa Barbara, CA 93106, USA

ARTICLE INFO

Article history:
Received 14 March 2014
Received in revised form 13 June 2014
Accepted 30 June 2014
Available online 9 July 2014
This manuscript was handled by Geoff Syme, Editor-in-Chief

Keywords:
Surface water–groundwater interaction
Arid zone hydrology
Environmental tracers
Eco-hydrology
Transient storage model
Hyporheic exchange

SUMMARY

Hyporheic and parafluvial flows between streams and the underlying streambed, or adjacent alluvium, are important drivers of biogeochemical cycling in streams. Here we present a new method for characterising this exchange in a losing stream based on longitudinal stream radon activities. A mass balance approach is used to constrain the radon influx into the stream and estimate exchange parameters: flux, residence time and exchange zone thickness. A net radon flux into the stream of 5.4×10^4 Bq m^{-1} d^{-1} is required to balance radon losses to groundwater recharge, gas transfer and radioactive decay. Given the radon production rate of the sediments (1.3 ± 0.7 Bq L^{-1} d^{-1}), the minimum volume of alluvium flushed by either hyporheic or parafluvial exchange is 168 m^3 per m length of stream. Based on the stream width, depth of alluvial sediments and porosity, this implies that the exchange zone extends beneath the stream and an additional 11 m either side. The results of this new method are compared to two existing methods; streambed radon disequilibrium and transient storage modelling of breakthrough curves of an injected tracer. The stream radon mass balance provides a relatively simple means of estimating hyporheic (and parafluvial) exchange over tens to hundreds of kilometres of stream. Concurrent application of the stream radon method, transient storage modelling of injected tracer breakthrough curves and hydraulic methods is recommended to capture the full spectrum of hyporheic exchange in losing streams.

1. Introduction

Hyporheic exchange exerts an important influence on nutrient distribution, productivity and contaminant transport in streams (Bencala, 1984; Boulton et al., 2010; Findlay, 1995; Jones and Mulholland, 2000). While definitions of hyporheic exchange vary, the term generally refers to the cycling of water between a stream and the groundwater below and adjacent to it, creating an exchange zone with chemical properties that are different to both the stream and the aquifer. This cycling occurs at a range of scales and can be related to stream bed-forms, turbulent eddies, gravel bars and meanders (Boano et al., 2011; Cardenas et al., 2004; O'Connor and Harvey, 2008; Stonedahl et al., 2010).

A common technique for estimating hyporheic exchange is to inject a tracer into the stream and use a transient storage model to interpret the tracer breakthrough curves measured downstream (Bencala and Walters, 1983; Harvey and Wagner, 2000). Transient storage models were originally developed to represent exchange between the stream and one storage zone (e.g.), but have since been extended to represent exchange between the stream and multiple storage zones, (e.g. Choi et al. (2000)). The time scale of tracer injection and measurement is usually on the order of hours with breakthrough curves measured at locations within one kilometre of the injection point. The sensitivity of the method is limited to flow paths on smaller spatial and temporal scales than the injection experiment. As a result, this scale of tracer injection usually captures fluxes with residence times of hours or less and spatial scales of hundreds of metres or less (Harvey et al., 1996). Although they remain widely used, recent studies have highlighted the non-uniqueness of transient storage model parameters (Kelleher et al., 2013), and the need for concurrent application of multiple methods, rather than a reliance on transient storage modelling alone (Ward et al., 2013).

Radon-222 (hereafter referred to as radon) is a radiogenic noble gas with a half-life of 3.8 days that is produced by most sediment through the decay of uranium series isotopes (Cecil and Green,

* Corresponding author. Address: University of Saskatchewan, Saskatoon, Canada.
E-mail address: sarah.bourke@usask.ca (S.A. Bourke).

http://dx.doi.org/10.1016/j.jhydrol.2014.06.057
0022-1694/

2000). Radon activity in surface water is low as radon is readily lost to the atmosphere through gas transfer. Water that enters the sub-surface increases in radon activity over a period of around 20 days until equilibrium between radon production and decay is reached. In losing streams, radon activity in groundwater has previously been used to infer rates of infiltration (Bertin and Bourg, 1994; Hoehn and Von Gunten, 1989). Disequilibrium of radon activities within the streambed has been used to infer residence times in the hyporheic zone (Lamontagne and Cook, 2007). Streambed radon activities are relatively easy to measure but interpretation of streambed radon profiles requires an estimate of the radon production rate of the sediments, which can be highly variable in heterogeneous alluvial sediments (Cecil and Green, 2000). Also, calculation of hyporheic fluxes from streambed radon activities requires an independent estimate of groundwater recharge or discharge.

In gaining stream systems, groundwater inflow rates and hyporheic exchange have been estimated based on stream radon activities using a 1D mass balance model (Cook et al., 2003, 2006). One of the major difficulties with this approach is separating the radon contribution through hyporheic exchange from the radon contribution of groundwater discharge.

In a losing stream where there is no groundwater discharge, the only influx of radon is through hyporheic exchange. As water enters the sub-surface hyporheic zone, the radon activity will increase with increasing hyporheic residence time. This radon is then introduced into the stream upon re-emergence of water from the hyporheic zone. The radon activity in the stream is therefore determined by the balance of losses to groundwater recharge, radioactive decay and gas transfer with the atmosphere, and additions through hyporheic exchange. If these loss terms are known, longitudinal stream radon activities in a losing stream can be used to estimate hyporheic exchange parameters (hyporheic zone depth, flux and residence time). In this paper we apply this new method for characterising hyporheic exchange parameters based on longitudinal stream radon activities in a losing stream. We then compare the results to estimates from two existing methods with differing scales of sensitivity: streambed radon disequilibrium and transient storage modelling of tracer breakthrough curves.

2. Theory

Definitions of hyporheic exchange are many and varied (Gooseff, 2010). Hydrochemically, the hyporheic zone can be considered as a zone where the interstitial water composition is a mixture of stream water and groundwater (Boulton et al., 2010; Hoehn and Cirpka, 2006; Triska et al., 1993). Hydrologists often define the hyporheic zone based on the extent of flow paths which originate from and return to the stream (O'Connor and Harvey, 2008; Stonedahl et al., 2010; Storey et al., 2003; Worman et al., 2002). In this context, hyporheic exchange can be considered to include a spectrum of flow paths ranging from shallow exchange between the stream and streambed on the scale of centimetres to longer return flows across stream meanders on the scale of tens to hundreds of metres (Stonedahl et al., 2010), without a clear boundary between these.

In this paper we find it useful to partition the total spectrum of hyporheic exchange into two components. We restrict our use of the term hyporheic exchange to refer to the relatively short flowpaths between the stream and streambed, characterised by residence times less than a day and spatial scales of tens of metres or less. This is the scale of hyporheic exchange that is most commonly to be captured by injected tracer experiments and streambed radon profiles. Exchange fluxes with longer residence times of days to weeks and spatial scales of tens to hundreds of metres are not commonly captured by injected tracer experiments, and are not well resolved by radon profiles beneath the streambed. These longer flow paths are often within the alluvium adjacent to the stream, and so we use the term parafluvial to refer to this exchange. Of course, these longer flow paths may also occur beneath the stream, flowing through the sub-surface approximately parallel to the direction of streamflow.

2.1. Stream radon activity

In a losing stream, the change in streamflow with distance is a function of groundwater recharge and evaporation, and is given by:

$$\frac{\partial Q}{\partial x} = -q_{gw} - Ew \tag{1}$$

where Q is the streamflow ($m^3\,d^{-1}$), q_{gw} is the groundwater recharge flux per metre length of stream ($m^2\,d^{-1}$), E is the evapotranspiration rate ($m\,d^{-1}$) and w is stream width (m). This groundwater recharge flux is related to the infiltration rate, I, of Cook et al. (2006) through the stream width: $q_{gw} = Iw$.

For dissolved gases like radon, gas transfer has a much greater than evaporation and therefore, the evaporation term can be neglected in the tracer mass balance. Cook et al. (2006) expressed the mass balance of radon in a losing stream as:

$$\frac{\partial Qc}{\partial x} = q_h(c_h - c) - q_{gw}c - kwc - \lambda dwc \tag{2}$$

where c is the radon activity within the stream, c_h is the radon activity within the hyporheic zone, q_h is the hyporheic exchange flux ($m^2\,d^{-1}$), k is the gas transfer velocity across the water surface ($m\,d^{-1}$), λ is the radioactive decay constant of radon ($0.181\,d^{-1}$), and d is the stream depth (m). Although this model does not explicitly include diffusion of radon from streambed sediments into the stream, this will be much smaller than the advective flux of radon associated with hyporheic exchange, and can be neglected.

Following Cook et al. (2006) and Lamontagne and Cook (2007), we model the hyporheic zone as a one-layer, uniform, well-mixed hyporheic zone. The steady state solute mass balance can be written:

$$q_h c - q_h c_h + q_{gw}c - q_{gw}c_h - \lambda wh\theta c_h + \gamma wh\theta = 0 \tag{3}$$

where h is the hyporheic zone depth (m), γ is the radon production rate of the sediments ($Bq\,L^{-1}\,d^{-1}$) and θ is porosity (Lamontagne and Cook, 2007). This conceptual model implies an exponential distribution of hyporheic residence times with a mean residence time, t_h (d) given by:

$$t_h = \frac{wh\theta}{(q_h + q_{gw})} \tag{4}$$

The concentration of radon within the hyporheic zone (c_h) will increase as the hyporheic zone residence time (t_h) increases, and hence the sensitivity of stream radon concentrations (c) to the hyporheic exchange flux (q_h) increases as the residence time (t_h) increases. Therefore, when the hyporheic exchange flow field includes both very short (fast) and very long (slow) flowpaths, it may be useful to explicitly differentiate between them. The mass balance of radon in the stream therefore becomes:

$$\frac{\partial Qc}{\partial x} = q_h(c_h - c) + q_p(c_p - c) - q_{gw}c - kwc - \lambda dwc \tag{5}$$

where q_p is the fluid flux in or out of the parafluvial zone ($m^2\,d^{-1}$), and c_p is the concentration of water discharging from the parafluvial zone into the stream.

The exponential distribution of travel times implied by Eq. (3) has been widely implemented in transient storage models (Bencala and Walters, 1983; Harvey et al., 1996; Runkel, 1998). Fig. 1 compares the effect of residence time distribution on the

radon flux from the hyporheic zone into the river. If the mean residence time in the hyporheic zone is less than 1 day, then the difference between these models is less than 10%, and so the form of the distribution is unimportant. However, the sensitivity to residence time distribution is greater (between 10% and 25% difference in radon flux) for residence times between 1 and 50 days. The exponential distribution is less likely to be less appropriate for longer flowpaths which may travel some lateral distance from the stream. We therefore represent parafluvial flowpaths as streamtubes, originating and ending in the stream, so that the radon activity of water leaving the parafluvial zone, c_p, is given by:

$$c_p = c_e - (c_e - c)e^{(-\lambda t_p)} \tag{6}$$

where t_p (d) is the parafluvial residence time and c_e (Bq L^{-1}) is the equilibrium radon activity. (This is equivalent to the piston flow model depicted in Fig. 1.) The equilibrium activity is related to the radon production rate, γ, by the relationship:

$$C_e = \frac{\gamma}{\lambda} \tag{7}$$

For any combination of parafluvial flux and residence time the total volume of alluvium flushed by parafluvial flow paths into each metre length of stream can be calculated from:

$$V_p = \frac{q_p t_p}{\theta} \tag{8}$$

where V_p is the volume flushed into each metre length of stream (m^2). V_p can be envisaged as the cross-sectional area of the parafluvial exchange zone.

Applying the chain rule of differentiation using Eqs. (1) and (5), substituting for c_h using Eqs. (3) and (4), and substituting for c_p using Eqs. (6) and (7), the change in radon activity along the stream can be expressed as:

$$Q\frac{\partial c}{dx} = \left(\frac{\gamma}{\lambda} - c\right)\left(\frac{q_h t_h}{\lambda^{-1} + t_h}\right) + \left(\frac{\gamma}{\lambda} - c\right)q_p(1 - e^{-\lambda t_p}) - kwc - \lambda dwc \tag{9}$$

where the first term on the right hand side denotes the change in concentration due to hyporheic exchange and the second term denotes parafluvial exchange. This equation can be used to constrain the radon flux entering the stream through exchange with streambed hyporheic and parafluvial zones based on measurements of stream radon activity.

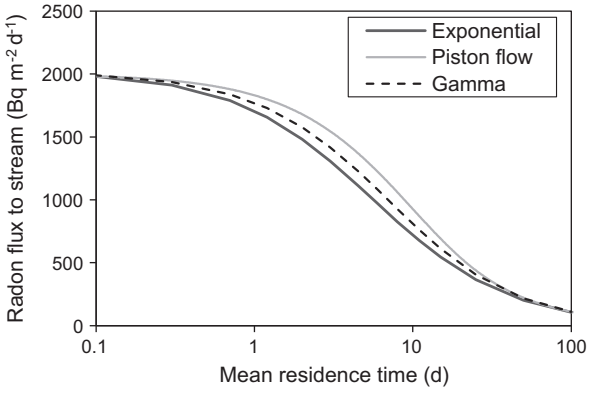

Fig. 1. Effect of residence time distribution of water within the hyporheic zone on the radon flux from the hyporheic zone to the river. The exponential distribution is assumed by the OTIS model, and was also used by Cook et al. (2006) and Lamontagne and Cook (2007). The piston flow model assumes that all water leaving the hyporheic zone has a residence time equal to the mean value. The gamma distribution assumes a coefficient of variation of 0.7. Simulations assume a hyporheic zone production rate of γ = 2 Bq/L/day, and thickness of h = 1 m, and negligible radon activity within the river.

2.2. Streambed radon disequilibrium

Estimates of hyporheic residence time can be made from vertical profiles of radon activity through the hyporheic zone. Rearranging Eq. (4) to solve for q_h and substituting this into Eq. (3) gives:

$$t_h = \frac{c - c_h}{\lambda c_h - \gamma} \tag{10}$$

which can be used to estimate hyporheic residence times based on measurements of stream radon activity, hyporheic radon activity and the radon production rate of the sediments (Lamontagne and Cook, 2007). Once this residence time has been calculated, if the groundwater recharge flux, q_{gw}, is also known, the hyporheic flux can be calculated by rearranging Eq. (4) to solve for q_h.

2.3. Transient storage modelling

The breakthrough curves of a conservative artificial tracer can be interpreted using a transient storage model to infer the exchange flux between the stream and storage zone (Bencala and Walters, 1983; Harvey et al., 1996). While this exchange flux is sometimes equated with streambed hyporheic exchange it also includes parafluvial flow and the effects of stagnant zones along the stream channel that retard solute transport. In this paper we use OTIS to interpret tracer breakthrough curves (Runkel, 1998). This model assumes that solute concentrations vary only in the longitudinal direction, mass is conserved within the stream and storage zone, and transient storage is the only physical process affecting solute concentrations within the storage zone. In the absence of decay, sorption or lateral inflow, the concentration of solute in the stream channel and storage zone are described by:

$$\frac{\partial c}{\partial t} = -\frac{Q}{A}\frac{\partial c}{\partial x} + \frac{1}{A}\frac{\partial}{\partial x}\left(AD\frac{\partial c}{\partial x}\right) + \alpha(c_s - c) \tag{11}$$

$$\frac{\partial c_s}{\partial t} = -\frac{A}{A_s}(\alpha(c_s - c)) \tag{12}$$

where c is the solute concentration in the stream (mg L^{-1}), Q is the volumetric flow rate (m^3 s^{-1}), D is the dispersion coefficient (m^2 s^{-1}), A is the cross sectional area of the channel (m^2), c_s is the solute concentration in the storage zone (mg L^{-1}), A_s is the cross-sectional area of the storage zone (m^2) and α is the storage exchange coefficient (s^{-1}). The flux between the stream and the storage zone (q_s, m^2 s^{-1}) and the mean residence time (t_s, s) within the storage zone can be calculated from:

$$q_s = \alpha A \tag{13}$$

$$t_s = \frac{A_s}{\alpha A} \tag{14}$$

3. Site description

Marillana Creek is a naturally ephemeral stream in the arid subtropical Pilbara region of Western Australia (Fig. 2). The creek flows north east across the Hammersley Basin into the Fortescue Marsh, approximately 40 km downstream of the study site. The creek flows adjacent to a series of iron ore mines that produce excess mine water during dewatering operations. In addition to natural episodic flow events, around 6 GL of mine water has been discharged to the creek each year, for 13 years prior to this study. The alluvial deposit associated with Marillana Creek is between 50 and 300 m wide and approximately 5 m thick. The streambed

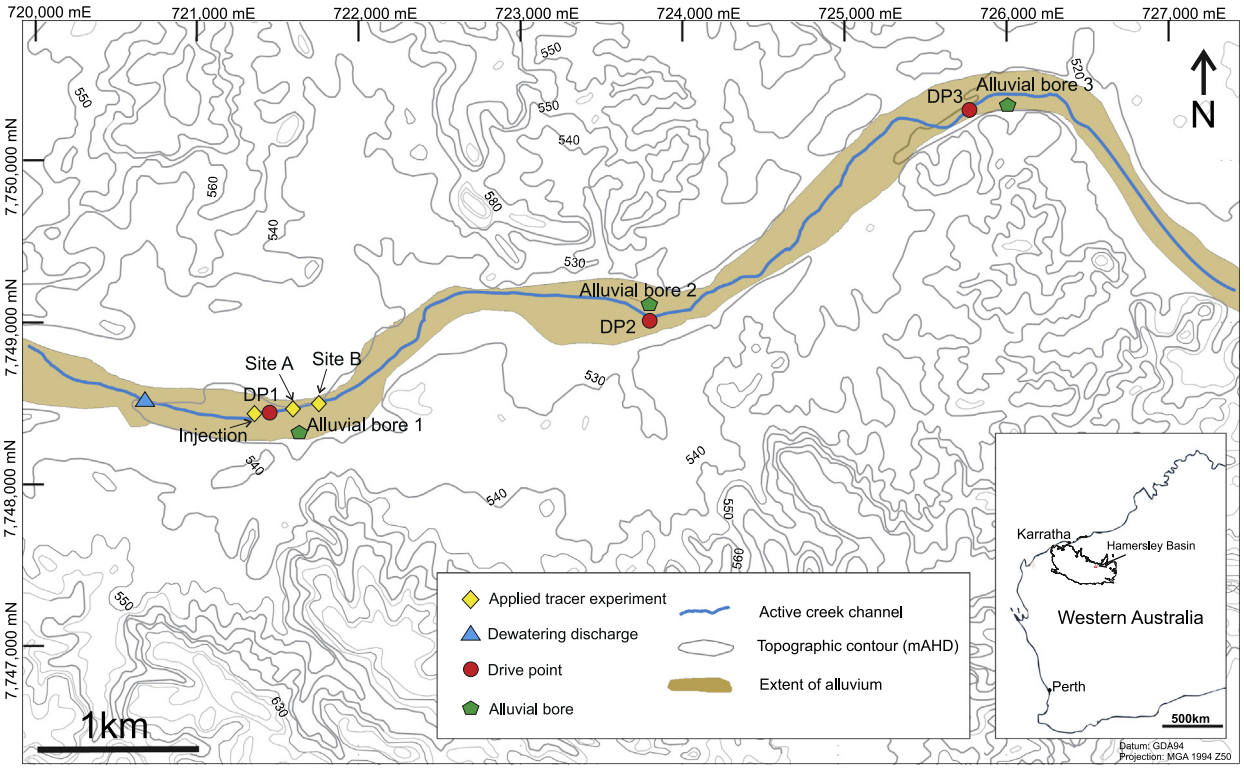

Fig. 2. Map of the study site showing tracer injection, DP1, 2, 3 and alluvial bore locations. Arrow in locality map points to study site within Hamersley Basin. Streamflow is from west to east (left to right).

(alluvium directly underneath the flowing stream) is not distinct from the alluvium adjacent to, or further below the stream (by visual inspection) and the stream channel is not significantly incised into the broader alluvial channel. The hydraulic conductivity of this alluvium has been estimated at between 1500 and 3700 m d^{-1}, based on pit infiltration tests. This alluvial deposit is predominantly underlain by a palaeochannel deposit of fractured pisolitic goethite (Ramanaidou et al., 2003) that extends to a depth of up to 50 m, with a hydraulic conductivity on the order of 10 m d^{-1}. Where the paleochannel deposit is absent, the creek alluvium is underlain by variably weathered, impermeable basement rock (Weeli Wolli formation), which consists of banded iron formation (BIF), chert and dolerite.

This study focuses on an 8 km long section of Marillana Creek immediately downstream of the mine water injection point. Streamflow at the discharge location is on the order of 0.3 m^3 s^{-1} and is relatively constant throughout the year (data not presented). Streamflow decreases along the 8 km section until there is no longer continuous flow, and the surface water expression is reduced to a series of disconnected pools. Along the study reach the stream is hydraulically connected to the Stream stage is approximately 1 m above the water table in the alluvial aquifer, based on measurements in piezometers between 80 and 120 m from the stream (Fig. 3). Thus, while the stream is clearly losing on a regional scale, this does not prohibit smaller scale exchange between the river and the adjacent alluvium, and the relationship between stream stage and aquifer hydraulic head on a smaller scale is likely to be quite complex. Similarly, the stream stage is 3 m above the hydraulic head in the underlying fractured bedrock aquifer.

The stream geomorphology is characterised by sequences of pools, riffles and glides. The majority of the 8 km section consists of glides; on average 0.5 m deep and ranging from 5 to 20 m wide. These glides are separated by riffles 5 m wide and up to 0.3 m deep and 10 m long. Pools are less than 5 m long and up to 1 m deep. In this paper, all river distances refer to distances downstream of the dewatering discharge location.

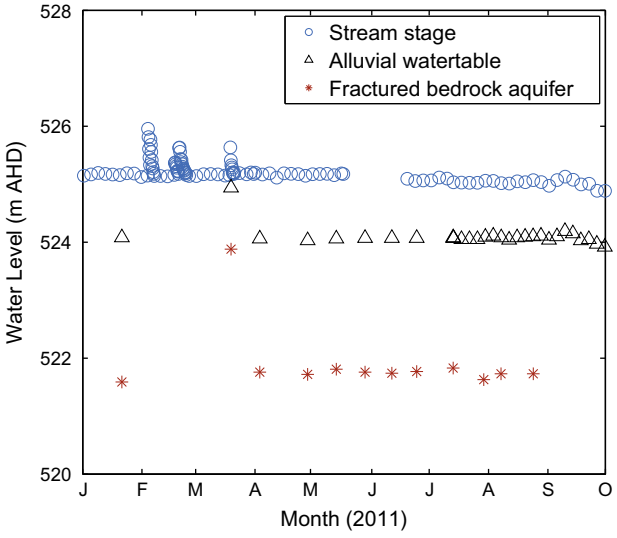

Fig. 3. Stream stage and hydraulic head in the alluvial aquifer (Alluvial bore 1), and the fractured goethite aquifer directly below.

4. Methods

4.1. Radon production rate

We used two methods to estimate the radon production rate of the sediments; water samples from alluvial bores and an incubation experiment (following a method similar to Corbett

et al. (1998)). These methods provide estimates of equilibrium activity, which provide the basis for estimates of radon production rates (according to Eq. (7)). Water samples were collected from pre-existing wells screened across the watertable within the alluvium close to sites DP1, DP2 and DP3 (see Fig. 2). For the incubation experiment, sediment samples were collected from 5 sites along the creek at river distances of 0.3, 1.0, 2.2, 3.5 and 6.1 km. At each of these sites, sediment was collected from; (a) the sediment–water interface (SWI), (b) 0.5 m below the SWI, and (c) the dry alluvium adjacent to the stream, giving a total of 15 sediment samples. Porosity was measured volumetrically and bulk density calculated as the dry weight per total volume. Three split replicates from each sediment sample were then saturated with deionized water in sealed 500 mL glass jars (45 jars total) and allowed to reach an equilibrium radon activity over 29 days. Radon activities of the water were then determined based on 14 mL sub-samples. The radon activity of these samples was determined by liquid scintillation using a LKB Wallace Quantulus counter. The accuracy of this method varies with concentration, and in this study ranged from ±0.15 Bq L^{-1} at a concentration of 2.7 Bq L^{-1} to ±0.5 Bq L^{-1} at a concentration of 19.5 Bq L^{-1} with a precision of approximately ±0.3 Bq L^{-1} (Leaney and Herczeg, 2006).

4.2. Longitudinal stream radon

Stream radon activity was measured at 12 sites along the stream between 17 and 19 May 2011, including directly from the mine water outlet. An additional stream sampling campaign was undertaken on 24–25 August 2011, during which water samples were collected at the mine water outlet and 18 sites along the stream approximately 500 m apart. Surface water samples for radon were initially collected in 1250 mL PET bottles. A 50 mL volume was removed from the bottle and 20 mL of mineral oil scintillant was added. The bottle was then shaken for 4 min before the scintillant oil was extracted into a pre-weighed PTFE scintillation vial. Radon activity was then determined by liquid scintillation as described in Section 4.1.

Stream velocity was measured on 23 August at 4 locations along the creek using an electromagnetic flow meter (Flowmate 2000). Streamflow was calculated by integrating flow measurements recorded at 0.25 m intervals across the width of the stream following the method of Buchanan and Somers (1969). The locations of these measurements coincide with the mine water discharge outlet, and locations DP1, DP2, and DP3 shown on Fig. 2. The location of the end of flow was also determined.

A tracer injection of sulphur hexafluoride (SF_6) was conducted at the same location as the bromide injection on 25–26 August 2011 to estimate the gas transfer velocity (Wanninkhof et al., 1987). The SF_6 gas was released by diffusion through nylon tubing connected to a gas cylinder supplying an outlet pressure of 90 kPa, following the procedure of Cook et al. (2006). The gas was released continuously for 60 h until sampling was complete. Water samples were collected in 15 mL Vacutainers at 8 locations over the 7 km downstream of the injection point. The first sample was collected 40 h after the injection commenced, to allow stream concentrations to first reach equilibrium. If the SF_6 release was not long enough for the stream concentrations to have reached equilibrium, then the estimated gas transfer rate would be too large. We therefore conducted a longer SF_6 injection on 5–9 October 2012, during which samples were not collected for the first 5 days. Streamflow during this second experiment was comparable to the August 2011 release. SF_6 concentrations were measured using the modified Vacutainer headspace method developed by Clark et al. (2004) on a gas chromatograph equipped with an Electron Capture Detector.

A 1D mass balance model of stream chemistry was built in EXCEL to interpret the longitudinal stream chemistry data. This model explicitly solves the mass balance equation by finite difference approximation with a spatial discretization of 10 m. This model was be used to simulate chloride concentration, SF_6 concentration and radon activity along the stream. Parameters used in the mass balance model are summarized in Table 1. Stream geometry was held constant along the entire model with a width of 12 m and a depth of 0.5 m. These are average values along the 8 km of stream that are simulated, based on field measurements and interpretation of aerial photographs. Streamflow losses to infiltration and evapotranspiration are constrained by fitting measured streamflow and chloride in the 1D mass balance model. The infiltration and evapotranspiration rates were constant along the entire model domain at values that provided the best fit to the streamflow and chloride data. The gas transfer rate was determined from the best fit to data from the SF_6 injection experiment. The radon production rate of the sediments was chosen to represent the mean production rate based on the incubation experiment and water samples from bores screened within the alluvium. A sensitivity analysis was conducted on the 1D mass balance model by adjusting individual parameters to ±50% of the best-fit value, while holding all other parameters constant.

Uncertainty in the calculated parafluvial exchange flux and volume was estimated using a Monte Carlo approach (10,000 realizations). The equilibrium radon activity is assumed to be log-normally distributed and was described by a normal distribution with a mean of 2.1 Bq L^{-1} d^{-1} and a standard deviation of 0.06 Bq L^{-1} d^{-1}. This mean is calculated from the natural log of the measured mean equilibrium radon activity (see Sections 4.1 and 4.2). The standard deviation represents the standard deviation of the mean, and is calculated from $0.46/\sqrt{n}$, where 0.46 is the standard deviation of the log-normalized measured data, and n is the number of samples ($n = 52$). The gas transfer velocity is assumed to be normally distributed with a mean of 1.8 m d^{-1} and a standard deviation 0.4 m d^{-1} (20% of the mean). The resulting uncertainty in the volume flushed by parafluvial exchange is also a function of porosity, which was assumed to be normally distributed with a mean of 0.3 and standard deviation of 0.03 (10% of the mean).

Table 1
Mass balance model parameters.

Symbol	Description	Value	Units
Chloride			
E	Evapotranspiration rate	0.014	m d^{-1}
w	Stream width	12	m
d	Stream depth	0.5	m
SF_6			
E	Evapotranspiration rate	0.014	m d^{-1}
w	Stream width	12	m
d	Stream depth	0.5	m
k	Gas transfer velocity	1.8	m d^{-1}
Radon			
E	Evapotranspiration rate	0.014	m d^{-1}
w	Stream width	12	m
d	Stream depth	0.5	m
k	Gas transfer velocity	1.8	m d^{-1}
θ	Hyporheic zone porosity	0.3	v v^{-1}
λ	Radon decay constant	0.181	d^{-1}
γ	Radon production rate within hyporheic zone	1.5	Bq L^{-1} d^{-1}
q_{gw}	Groundwater recharge flux	2.6	m^2 d^{-1}
q_h	Hyporheic water flux		m^2 d^{-1}
q_p	Parafluvial water flux		m^2 d^{-1}
t_h	Hyporheic zone residence time		d
t_p	Residence time of parafluvial flow		d
v_p	Volume flushed by parafluvial flow		m^3 m^{-1}

4.3. Streambed radon profiles

Vertical profiles of streambed radon activity were measured on 24 August 2011 at three locations along the creek; DP1, DP2 and DP3, located at 950, 3750 and 6330 m, respectively. Pore water samples were collected to a depth of up to 1.2 m using a 30 mm outer diameter drive point and a 20 mL syringe to sample 14 mL of water from each depth. These water samples were injected through a 0.4 μm disposable inline filter into pre-weighed Teflon coated PTFE scintillation vials containing 6 mL of Packard NEN mineral oil. Radon activities were determined using liquid scintillation, as described in Section 4.1.

Hyporheic residence times were estimated from Eq. (10), based on the stream and hyporheic radon activities and the streambed radon production rate. Confidence bounds on hyporheic residence times were calculated using a Monte Carlo analysis that incorporated analytical measurement error and uncertainty in the radon production rate of the sediments. For each depth at each site, the distribution of porewater radon activity was assumed to be normally distributed with a mean given by the laboratory reported radon activity at that depth, and standard deviation given by the laboratory measurement error. The distribution of equilibrium activities at each site was assumed to follow a normal distribution described by the mean and standard deviation across incubation and bore water samples from each site (10.4 ± 4.0 Bq L^{-1} at DP1, 7.0 ± 1.6 Bq L^{-1} at DP2 and 7.0 ± 0.8 Bq L^{-1} at DP3). If the radon activity in the hyporheic zone (c_h) is less than the radon activity in the stream (c), the calculated hyporheic residence time (t_h) is negative. To account for this, during the Monte Carlo analysis, if the generated radon activity in the streambed was less than the activity in the stream, a residence time of zero days was assigned to that realisation. As a result, where there is significant overlap between the distributions of streambed and stream radon activity, the upper bound of the 90% confidence interval hyporheic residence time can be estimated, but not the lower bound. Similarly, where there is significant overlap between the streambed radon distribution and the equilibrium activity distribution, the lower bound of the 90% confidence interval of hyporheic residence time can be estimated, but not the upper bound.

4.4. Injected tracer and transient storage modelling

A tracer pulse of potassium bromide (KBr) was injected into the creek on 25 August 2011, at a river distance of 930 m. This tracer pulse consisted of approximately 40 L of water with a concentration of 72,000 mg L^{-1}, injected over 90 s. The injection location was chosen such that slow moving glides that might retard solute for hours or longer were not included in the experiment, and with a turbulent riffle between the point of injection and the first sampling station, to maximise solute mixing. Water samples were collected at two stations, 150 m (Site A) and 265 m (Site B) downstream of the injection point, over a 2 h period immediately following the tracer injection. Stream discharge at Site A was measured at 0.2 m^3 s^{-1} using an electromagnetic flow meter and was consistent throughout the experiment. In-situ measurements of electrical conductivity were also made at these stations throughout the experiment to inform sample collection. Bromide concentrations were measured by ion chromatography.

Bromide breakthrough curves from the applied tracer experiment were interpreted using the OTIS transient storage model (Runkel, 1998). The model consisted of one reach beginning at Site A and ending at Site B, 115 m in length. This reach was divided into 1 m long segments along the entire model domain. The time step was 1 min with a total simulation time of 2 h. A lateral outflow of 2.04×10^{-5} m^2 s^{-1} was applied along the entire model domain to simulate infiltration (groundwater recharge) at a rate of 0.22 m d^{-1}, with an average stream width of 8 m along the 115 m of stream. Streamflow at the upstream boundary was 0.2 m^3 s^{-1}. Concentrations at the upstream boundary were defined by measured data at sampling site A with linear interpolation between successive data points. The longitudinal dispersion coefficient (D), stream channel area (A) storage area (A_s) and storage exchange coefficient (α) were estimated using the inverse parameter estimation functionality of OTIS-P with a stopping value of 10^{-5} and unweighted residuals. The storage exchange flux and residence time were calculated from these parameters (A_s and α) using Eqs. (13) and (14).

5. Results

5.1. Radon production rate

Equilibrium activities in the alluvial wells were 8.0 ± 1.2 Bq L^{-1} ($n = 3$) at DP1, 6.7 ± 0.4 Bq L^{-1} ($n = 3$) at DP2 and 6.7 Bq L^{-1} ($n = 1$) at DP3 (all errors in this section are standard deviation). Production rates at each well, calculated from Eq. (7), were 1.5 ± 0.2 Bq L^{-1} d^{-1} at DP1, 1.2 ± 0.1 Bq L^{-1} d^{-1} at DP2, and 1.2 Bq L^{-1} d^{-1} at DP3. Equilibrium activities in the incubation tests ($n = 45$) ranged from 2.7 to 19.5 Bq L^{-1} with a mean activity of 6.8 ± 3.8 Bq L^{-1} and a median of 5.6 Bq L^{-1}. The equilibrium activity of incubation tests on sediment samples from DP1 was 11.15 ± 4.3 Bq L^{-1}, on sediment from DP2 was 4.4 ± 1.4 Bq L^{-1}, and on sediment from DP3 was 5.4 ± 0.8 Bq L^{-1}. Production rates calculated from these equilibrium activities were 2.0 ± 0.8 Bq L^{-1} d^{-1} at DP1, 0.8 ± 0.3 Bq L^{-1} d^{-1} at DP2, and 1.0 ± 0.1 Bq L^{-1} d^{-1} at DP3. Averaged across all samples including wells and incubation tests ($n = 52$), the equilibrium activity was 7.2 ± 3.8 Bq L^{-1}, which implies a production rate of 1.3 ± 0.7 Bq L^{-1} d^{-1}.

5.2. Streambed radon profiles

At site DP1, radon activities in the upper 0.1 m of the streambed ranged from 2.8 to 2.9 Bq L^{-1}, slightly higher than the radon activity of the stream, which was 2.4 Bq L^{-1} (Fig. 4). This suggests the presence of a rapidly flushed hyporheic zone in the upper 0.1 m of streambed at this site. In contrast, radon activities below 0.1 m at DP1, and throughout the profiles at DP2 and DP3 ranged from 3.9 to 8.7 Bq L^{-1}, suggesting residence times of days (Eq. (10)).

The median residence time within the upper 0.1 m at DP1 was 0.3 days, with a 90% confidence interval of 0–3 days (Fig. 4b). Below 0.1 m the median residence times generally increased with depth from 6.3 days to 19.2 days, with the lower bounds of the 90% confidence intervals from 2.2 to 4.1 days. Median residence times were between 1.7 and 9.5 days at site DP2, and between 2.7 and 11.1 days at DP3. These data imply that at sites DP2 and DP3 the rapidly flushed hyporheic zone is either absent, or shallower than the 0.05 m sampling interval at the top of each profile. Hyporheic exchange fluxes can theoretically be estimated based on the residence time using Eq. (4), if the groundwater recharge flux and hyporheic zone geometry are known. However, when the uncertainty in hyporheic residence times is considered, calculated flux estimates are effectively unbounded.

5.3. Injected tracer and transient storage modelling

During the injected tracer experiment bromide concentrations increased from a background concentration of 0.5 mg L^{-1} up to a peak of 35 mg L^{-1} at Site A approximately 10 min after the tracer injection (Fig. 5). At site B the concentration peaked at 14 mg L^{-1} approximately 35 min after tracer injection. Integration of the bromide breakthrough curves showed that mass recovered at station B

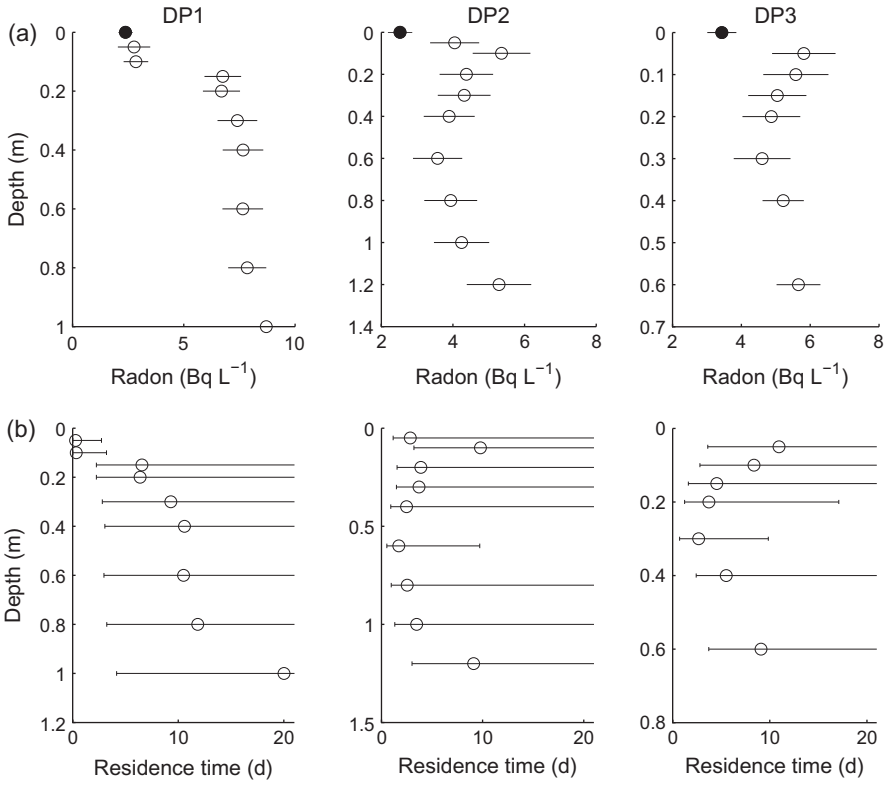

Fig. 4. (a) Streambed radon profiles. Dark circles are surface water samples, open circles are subsurface water samples. Error bars are 2σ based on laboratory measurement uncertainty. (b) Median hyporheic residence time and 90% confidence interval based on Monte Carlo analysis.

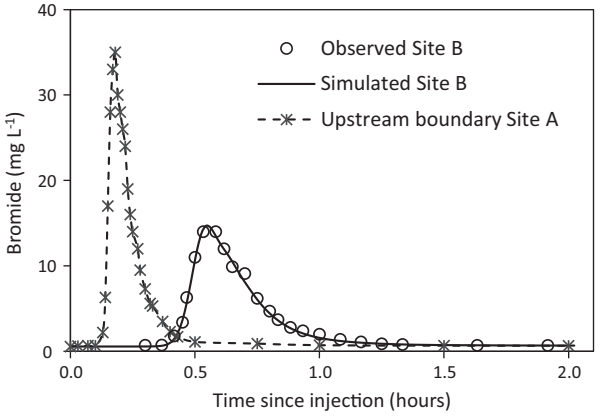

Fig. 5. Bromide concentrations measured at site A and B, upstream boundary (linear interpolation of site A measured data) and OTIS simulated bromide concentration at site B.

was 97.8% of the total mass at station A (the upstream model boundary). Losses to infiltration between stations A and B accounted for 1.2% of this mass loss (33 g), leaving 1.0% of the mass (30 g) as remaining in the storage zone at the end of the 2 h simulation period.

OTIS-P converged on a solution for all four parameters, with an RMSE of 0.3 Bq L^{-1} and an R^2 value of 0.99. Stream channel area, storage area and the storage exchange coefficient were well constrained (Table 2). The stream channel area was estimated at 2.0 ± 0.1 m^2, the storage area estimated at 0.6 ± 0.1 m^2 and the storage exchange coefficient was estimated at $1.3 \times 10^{-3} \pm 4 \times 10^{-4}$ s^{-1} (95% confidence limits). The longitudinal dispersion coefficient (D) was the least well constrained parameter, estimated at $3.8 \times 10^{-2} \pm 2.8 \times 10^{-2}$ m^2 s^{-1}. Fluid flux between the stream channel and storage zone, was calculated based on Eq. (13), giving an estimated storage flux (q_s) of $2.6 \times 10^{-3} \pm 0.4 \times 10^{-3}$ m^2 s^{-1} (225 ± 35 m^2 d^{-1}). The average turnover rate, or mean residence time within this storage zone (t_s) was calculated by Eq. (14), to be 230 ± 40 s (approximately 4 min or 0.003 days). The transient storage modelling approach simulates an exponential distribution of residence times within the storage zone. Therefore, this mean of 4 min corresponds to an exponential distribution of residence times with 90% of residence times less than 10 min (0.007 days) and 99.9% of residence times less than 28 min (0.02 days). If we assume exchange with stagnant pools to be negligible, the storage

Table 2
OTIS-P parameter estimates.

Model parameter	Units	Parameter estimate	Standard deviation
Longitudinal dispersion coefficient (D)	m^2 s^{-1}	3.8×10^{-2}	1.3×10^{-2}
Stream channel area (A)	m^2	2.0	4.1×10^{-2}
Storage area (A_s)	m^2	0.6	4.0×10^{-2}
Storage exchange coefficient (α)	s^{-1}	1.3×10^{-3}	2.1×10^{-4}
Storage exchange flux (q_s)	m^2 s^{-1}	2.6×10^{-3}	4.2×10^{-4}
Storage zone residence time (t_s)	s	230	40

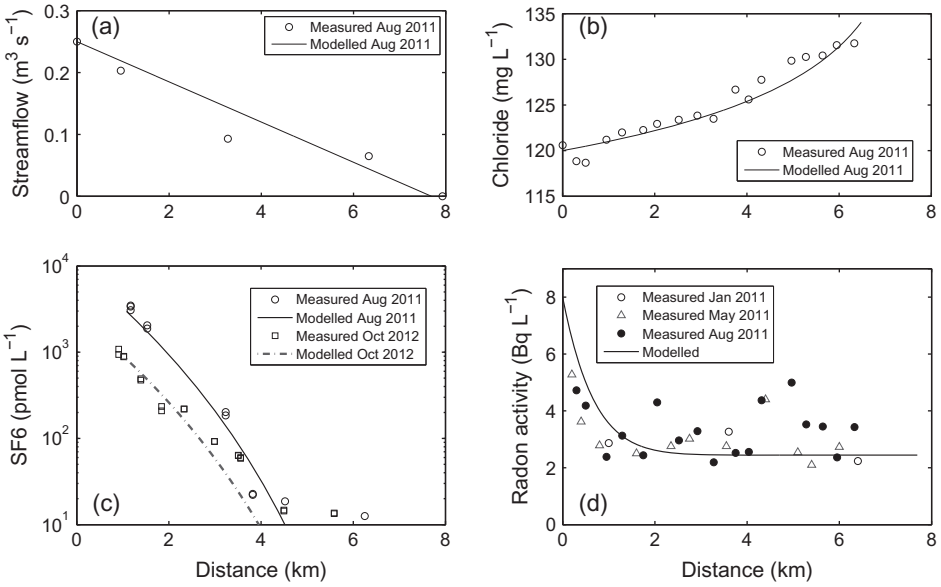

Fig. 6. Measured and modelled (a) streamflow, (b) chloride, (c) SF_6 and (d) radon activity. Distances are downstream of the mine water outlet.

area of 0.6 m^2 implies a storage zone depth of 0.25 m (based on stream width of 8 m and porosity of 0.3).

5.4. Longitudinal stream radon

At the time of the August sampling campaign, streamflow decreased from 0.25 $m^3\ s^{-1}$ at the mine water discharge outlet to effectively zero at a distance of 7900 m, where the surface water had reduced to a series of disconnected pools (Fig. 6). The chloride concentration increased along the stream from a minimum of 119 mg L^{-1} to 132 mg L^{-1}. Radon activities in the mine water discharge were 10.9 ± 0.6 Bq L^{-1} in May and 13.1 ± 0.7 Bq L^{-1} in August 2011. Flow at the discharge outlet was fast and highly turbulent. A pool of mine water was created immediately upstream of the mine water outlet so that the water flowing along the stream was likely to be a mixture of water from this pool and more recent mine water. As a result, stream radon activities immediately where the stream begins to flow are likely to be lower than the values measured directly from the mine water outlet. We have used an initial stream radon activity of 8 Bq L^{-1} in the mass balance model that accounts for the enhanced degassing at the outlet location. Radon activities decreased to less than 5 Bq L^{-1} within 500 m downstream of the mine water discharge outlet. Radon activities along the subsequent 7400 m were between 2.0 and 4.9 Bq L^{-1} with an average of 3.3 ± 0.9 Bq L^{-1} (± std. dev.).

The groundwater recharge flux and evaporation rate were determined from the simulation of streamflow and chloride using the 1D mass balance model (see Section 4.2). The visual best fit to the observed data was achieved with a groundwater recharge flux of 2.6 $m^2\ d^{-1}$ and an evapotranspiration rate of 0.014 m d^{-1}. Pan evaporation measured by the Australian Bureau of Meteorology during the sampling period and evaporation estimates based on the Penman–Monteith equation both suggest evaporation rates on the order of 0.01 m d^{-1}. We therefore consider the simulated evapotranspiration rate to be reasonable with the excess above 0.01 m d^{-1} potentially attributable to transpiration by riparian vegetation. Given a mean stream width of 12 m, the best fit to the SF_6 data was achieved with a gas transfer rate of 1.8 m d^{-1}. This is consistent with previous stream radon studies that have used values of 1–1.6 m d^{-1} (Cook et al., 2003, 2006) and lies within the mid-range of literature values (Raymond and Cole, 2001).

In the absence of streambed hyporheic and parafluvial fluxes, the stream radon activity would reduce to zero within 3.5 km of the mine water outlet. In order to maintain a stream radon activity of 2.4 Bq L^{-1} downstream of 3.5 km, a radon flux of 5.4×10^4 Bq $m^{-1}\ d^{-1}$ is required to balance radon losses to groundwater recharge, gas transfer and radioactive decay. This radon flux must be derived from either hyporheic or parafluvial exchange or a combination of the two. However, without other information it is not possible to differentiate between them.

The hyporheic zone depth that would be required to maintain the estimated radon flux in the absence of parafluvial exchange is calculated by setting $\left(\frac{\gamma}{\lambda} - c\right)\left(\frac{q_h t_h}{\lambda^{-1} + t_h}\right) = 5.4 \times 10^4$ Bq $m^{-1}\ d^{-1}$ in Eq. (9) and substituting for q_h using Eq. (4). This gives a hyporheic zone depth, h, of greater than 14 m. (The smallest possible value of h is obtained when t_h is small. Larger values of t_h give larger values of h.) Thus, if the parafluvial flux were zero, a hyporheic zone at least 14 m thick (hyporheic zone volume of 168 m^2, based on a stream width of 12 m) would be required to sustain stream radon activities of 2.4 Bq L^{-1} downstream of 3.5 km from the mine water discharge outlet. This implied hyporheic zone depth is greater than the thickness of the alluvial deposit associated with the creek (approximately 5 m).

Alternatively, if hyporheic exchange is zero, then we can calculate the magnitude of parafluvial flow required to maintain the same radon flux. Thus setting $\left(\frac{\gamma}{\lambda}\right) q_p (1 - e^{-\lambda t_p}) = 5.4 \times 10^4$ Bq $m^{-1}\ d^{-1}$ and substituting for q_p using Eq. (8) gives $V_p > 170\ m^2$. (Again, the smallest possible value of V_p is associated with small values of t_h.) This value of V_p is effectively equivalent to the cross-sectional area of the parafluvial zone. Given that the alluvial channel is approximately 5 m deep, this suggests that the combined exchange zone is at least 34 m wide, extending beneath the stream (12 m wide) and an additional 11 m either side.

Although the minimum volume of alluvium flushed by either hyporheic or parafluvial exchange is 168 $m^3\ m^{-1}$, the precise volume flushed and the hyporheic and parafluvial fluxes are a function of the partitioning between the two exchanges and their respective mean residence times. As the residence times increases, the volume of sediment required to be flushed also increases. If we limit hyporheic exchange to depths of up to 3 m and residence times up to 2 days, then given a parafluvial residence time of 5 days, the corresponding volume flushed by parafluvial flow paths would be

between 202 and 258 $m^3 m^{-1}$. If the parafluvial residence time is longer, then a much larger parafluvial volume is required (Fig. 7).

If we assume that the hyporheic exchange flux is negligible, we can rearrange Eq. (9) to solve for the parafluvial flux, based on a given parafluvial residence time (when the stream radon activity is constant, the left hand side of Eq. (9) becomes zero). Uncertainty in the calculated parafluvial exchange flux and volume has been assessed using a Monte Carlo approach to calculated means and 90% confidence intervals (Section 4.2). For a parafluvial residence time of 5 days, if we consider only uncertainty in the mean equilibrium activity of the sediment, we get a mean parafluvial flux of 15.5 $m^2 d^{-1}$, with 90% confidence interval of 13.6–18.0 $m^2 d^{-1}$. If we also incorporate uncertainty in the gas transfer velocity, the 90% confidence interval expands to 10.0–21.8 $m^2 d^{-1}$. The corresponding volume of alluvium flushed, incorporating uncertainty in porosity, has a mean of 264 $m^3 m^{-1}$with a 90% confidence interval of 161–380 $m^3 m^{-1}$.

Simulated stream radon activities were most sensitive to the equilibrium activity and gas transfer rate (Fig. 8a and b). The radon production rate in the model was constrained by measuring the equilibrium activities of the incubation experiment and alluvial bores (see Section 5.1). Total losses through gas transfer are a function of both the gas transfer velocity and stream width. These parameters were constrained by measuring stream width at multiple locations along the study reach and conducting an SF_6 tracer injection to measure the gas transfer velocity. Simulated radon activity is only sensitive to initial radon activity in the upstream 2 km of the simulation. Radon simulations are not sensitive to infiltration or evapotranspiration rates (data not shown).

6. Discussion

Our ability to characterise the hyporheic zone is explicitly linked to the scale of sensitivity of the method that we apply, whether it is an environmental tracer, applied tracer experiment or a hydraulic approach (eg. Darcy's law, numerical modelling). In this paper we have chosen to distinguish between (1) short residence time, short flow path hyporheic fluxes that exchange water mostly between the stream and streambed, and (2) long residence time, long flow path, parafluvial fluxes flowing through the alluvium adjacent to or beneath the stream. This distinction has been made to reflect the temporal and spatial sensitivities of the methods used, and because the assumption of a uniform radon concentration (i.e. a well-mixed hyporheic zone) is not realistic for long-path exchange fluxes.

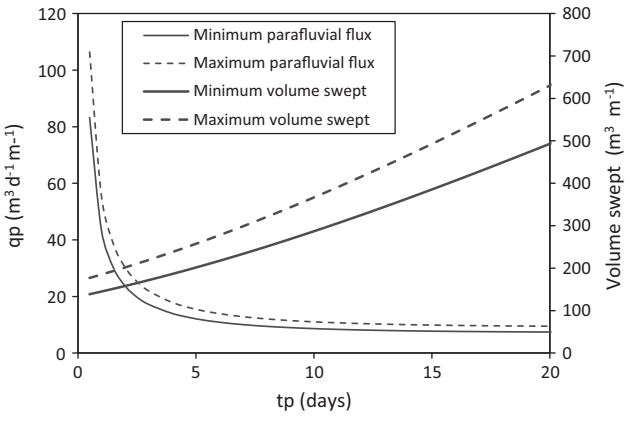

Fig. 7. Parafluvial fluxes and corresponding volume of alluvium flushed into each metre length of stream ($m^3 m^{-1}$) required to maintain radon activity in the stream at 2.4 Bq L^{-1} as a function of parafluvial residence time. The minimum volume flushed assumes the hyporheic zone is 3 m deep with a mean residence time of 0.001 days. The maximum volume flushed assumes hyporheic radon flux is negligible.

The longitudinal radon mass balance identified a parafluvial exchange zone extending to a distance of tens of metres from the stream. Detailed measurements of the local-scale head distribution within the alluvial aquifer would provide a means of validating these results. This scale of exchange is consistent with estimates from other field sites that have inferred parafluvial flow paths on spatial scales of tens to hundreds of metres and residence times of days or greater based on tracer injection (Dent et al., 2007; Holmes et al., 1994; Triska et al., 1993), nutrient distributions (Lewis et al., 2007), dissolved oxygen (Deforet et al., 2009), stable isotopes (Gooseff et al., 2003) and hydraulic gradients (Deforet et al., 2009; Peterson and Sickbert, 2006). The main advantage of the longitudinal radon mass balance approach over previous methods is that it can be implemented relatively easily over tens to hundreds of kilometres of stream. This method could also be applied in gaining streams, if an independent estimate of groundwater discharge to the stream was available.

Our estimates of the volume of sediments flushed are relatively insensitive to the assumed partitioning between the hyporheic and parafluvial zones and the residence time distribution assumed for each zone. Even at a very crude level, the absolute minimum volume of the combined hyporheic and parafluvial exchange zones required to generate the required radon influx to the stream can be calculated from the ratio between net radon flux into the stream necessary to maintain the measured radon activity (5.4×10^4 Bq $m^{-1} d^{-1}$) and the production rate within the sediments (1.5 Bq L^{-1} day^{-1}). This gives a minimum volume of water within the combined exchange zone of 36 m^3 per metre length of stream. The volume of aquifer of this combined exchange zone is then obtained by simply dividing by the porosity (0.3), giving 120 m^3 per metre length of stream. This estimate of the exchange zone volume (which is independent of any assumption concerning residence time distribution) is much greater than was indicated by either the applied tracer test or the radon profiles. Furthermore, this simple calculation is an underestimate of the true volume because (1) it ignores the radon flux from the river into the hyporheic zone (i.e., it measures the gross flux to the stream, not the net flux), and (2) it assumes a subsurface residence time of zero (i.e., all radon that is produced enters the stream, and none decays within the subsurface). When radon flux into the hyporheic zone is considered, the minimum volume becomes 168 m^2. Calculation of the actual volume of alluvium flushed requires independent information on the mean subsurface residence time, and the residence time distribution.

While the longitudinal stream radon method captures hyporheic and parafluvial exchange at regional scales, on its own, the method is not able to explicitly differentiate between hyporheic and parafluvial fluxes. Nevertheless, if other methods can be used to put an upper limit on the hyporheic flux, then this method provides an estimate of the parafluvial exchange flux, which may be otherwise difficult to obtain. The sensitivity of stream radon concentrations to the exchange flux (q_h, or q_p) increases as subsurface residence time increases due to radon in-growth (up to a residence time of approximately 7 days). Therefore, the method is more sensitive to parafluvial exchange than hyporheic exchange.

For the radon disequilibrium method, the uncertainty in the radon production rate of the sediments is a significant limitation. As a result, the disequilibrium method was able to highlight the presence or absence of rapidly flushed zones beneath the stream, but was not able to constrain the hyporheic exchange flux between stream and streambed. Extensive replication would be required to extrapolate these point-scale estimates of hyporheic zone depth to the reach scale. At the larger scales of application of the stream radon method, the mass balance model was also sensitive to the radon production rate, which must be estimated for the method to be applied. However, the longitudinal stream radon simulation

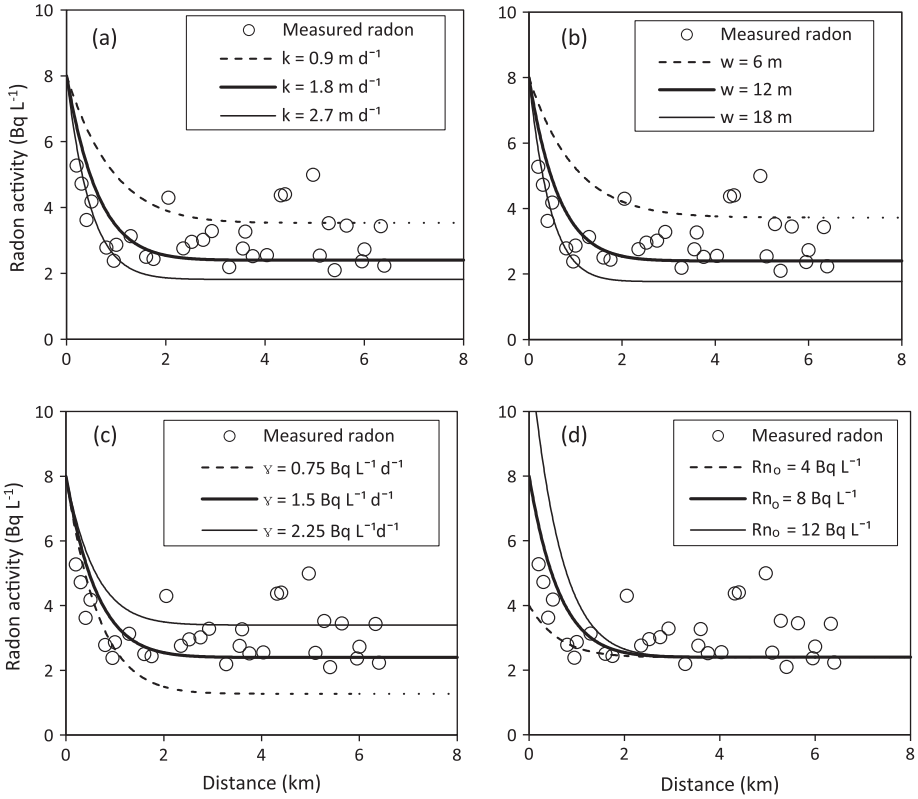

Fig. 8. Sensitivity of radon simulations to (a) gas transfer (k), (b) stream width (w) (c) radon production rate (γ) and (d) initial radon activity (Rn_0). Each parameter modelled at ±50% of base value.

is sensitive to the mean production rate along the entire model domain (8 km in this study). Therefore, it is less susceptible to heterogeneity in the radon production rate than the radon disequilibrium method, which requires estimates of radon production rate at each sample location (on the scale of centimetres).

Transient storage modelling of breakthrough curves captured the fastest exchange fluxes, with residence times of minutes and spatial scales less than 0.5 m. The storage flux estimate from transient storage modelling in this study was an order of magnitude larger than estimates of hyporheic flux in the literature, which are generally between 10^{-6} and $10^{-4}\,m^2\,s^{-1}$ (Bencala and Walters, 1983; Harvey et al., 1996; Lautz et al., 2010; Swanson and Cardenas, 2010). Stagnant zones were observed within the stream channel during the tracer injection and the relatively high storage flux measured in this study may reflect exchange with in-stream storage zones, rather than a sub-surface hyporheic zone (Jackson et al., 2012). Nevertheless, longer flowpath exchange fluxes would be expected to result in unattributed mass loss during the injected tracer experiment. This unattributed mass loss could provide an estimate of the magnitude of parafluvial exchange, without the underlying assumptions of the transient storage modelling approach. In this study, the tracer breakthrough curve does not suggest significant mass loss to parafluvial flow, with only 1% of the injected mass designated as unattributed losses over the 2 h sampling interval.

Although recent studies have highlighted limitations in the transient storage modelling approach for characterising hyporheic exchange (e.g. Kelleher et al. (2013) and Ward et al. (2013)), injected tracer experiments remain one of the few methods available to characterise hyporheic exchange on scales of hundreds of metres. A tracer injection experiment of longer duration than was applied in this study (days at least) would be required to resolve longer (parafluvial) exchange fluxes using a transient storage modelling approach. However, given that information on flow paths with long residence times can only be obtained from the tail of the breakthrough curve, it may be difficult to inject sufficient tracer to maintain concentrations above the detection limit throughout this sampling period.

Subsequent application of the longitudinal radon method in other losing streams, and in combination with more complex tracer injection methods (dilution gauging, estimates of gross gain and loss, eg. Payn et al. (2009)) should allow for stronger constraints on estimated residence times and fluxes. Application of a multi-zone transient storage model (e.g. Choi et al. (2000), Marion et al. (2008) and Briggs et al. (2009)), would allow for solute retention in the surface zone to be separated from solute retention in the hyporheic zone and potentially also the parafluvial zone, particularly if pore water samples were collected from the hyporheic zone during the experiment. Previous studies have reported that residence times within the hyporheic zone do not have an exponential distribution (an assumption which underlies the OTIS model) (Cardenas, 2008; Cardenas et al., 2004; Haggerty et al., 2002; Sawyer and Cardenas, 2009). Interpretation of breakthrough curves using a transient storage model that does not assume an exponential residence time distribution (e.g. Deng and Jung (2009), Boano et al. (2007)) may provide a more realistic representation of the physical distribution of residence times in the hyporheic zone.

Much of the interest in hyporheic exchange is due to its role in nutrient cycling in streams (Boano et al., 2010; Triska et al., 1993; Zarnetske et al., 2011). The extent of nutrient transformation is, in part, related to exchange zone residence time (Gomez et al., 2012; Zarnetske et al., 2011), which can vary over several orders of magnitude depending on hydraulic gradients and the permeability of the sediments (Findlay, 1995). Highly permeable sediments like the coarse alluvium in this study can result in shorter residence

times and therefore less potential for chemical and biological transformation (Claret and Boulton, 2009). However, the parafluvial zone in this system extends over tens of metres with a residence time of days. The significance of this exchange zone for biogeochemical transformation depends on the residence time relative to reaction rates, as described by the Damkohler number (Zarnetske et al., 2012). Local-scale measurement of the distributions of nutrients and dissolved organic matter would allow for the significance of hyporheic and parafluvial exchange in this stream system to be assessed (Zarnetske et al., 2011).

7. Conclusion

In this paper we present a new method for characterising hyporheic and parafluvial exchange in losing streams based on longitudinal stream radon activity. Based on the radon mass influx along an 8 km losing stream reach, we were able to estimate the volume of alluvium that must be flushed by hyporheic or parafluvial exchange. The major strength of the stream radon method is that it can provide an integrated measure of hyporheic and parafluvial exchange over kilometres of river. Furthermore, the stream radon method is most sensitive to exchange fluxes with long residence times and flow paths, which are not easily captured using pre-existing methods.

Acknowledgements

This work was undertaken as part of a collaborative project between the National Centre for Groundwater Research and Training (NCGRT) and Rio Tinto Iron Ore. The National Centre for Groundwater Research and Training is an Australian Government initiative supported by the Australian Research Council and the National Water Commission and CSIRO Water for a Healthy Country. The authors would like to thank Paul Hedley and Roger Cranswick for their assistance during the bromide injection experiment.

References

Bencala, K.E., 1984. Interactions of solutes and streambed sediment: 2. A dynamic analysis of coupled hydrologic and chemical processes that determine solute transport. Water Resour. Res. 20 (12), 1804–1814.
Bencala, K.E., Walters, R.A., 1983. Simulation of solute transport in a mountain pool-and-riffle stream: a transient storage model. Water Resour. Res. 19 (3), 718–724.
Bertin, C., Bourg, A., 1994. Radon-222 and chloride as natural tracers of the infiltration of river water into an alluvial aquifer in which there is significant river/groundwater mixing. Environ. Sci. Technol. 28 (5), 794–798.
Boano, F., Packman, A., Cortis, A., Revelli, R., Ridolfi, L., 2007. A continuous time random walk approach to the stream transport of solutes. Water Resour. Res. 43 (10).
Boano, F., Demaria, A., Revelli, R., Ridolfi, L., 2010. Biogeochemical zonation due to intrameander hyporheic flow. Water Resour. Res. 46 (2), W02511.
Boano, F., Revelli, R., Ridolfi, L., 2011. Water and solute exchange through flat streambeds induced by large turbulent eddies. J. Hydrol. 402 (3–4), 290–296.
Boulton, A.J., Datry, T., Kasahara, T., Mutz, M., Stanford, J.A., 2010. Ecology and management of the hyporheic zone: stream-groundwater interactions of running waters and their floodplains. J. North Am. Benthol. Soc. 29 (1), 26–40.
Briggs, M.A., Gooseff, M.N., Arp, C.D., Baker, M.A., 2009. A method for estimating surface transient storage parameters for streams with concurrent hyporheic storage. Water Resour. Res. 45 (4).
Buchanan, T.J., Somers, W.P., 1969. Discharge Measurements at Gaging Stations. US Government Printing Office, Washington, DC.
Cardenas, M.B., 2008. Surface water-groundwater interface geomorphology leads to scaling of residence times. Geophys. Res. Lett. 35 (8).
Cardenas, M.B., Wilson, J.L., Zlotnik, V.A., 2004. Impact of heterogeneity, bed forms, and stream curvature on subchannel hyporheic exchange. Water Resour. Res. 40, W08307.
Cecil, L.D., Green, J.R., 2000. Radon-222. In: Cook, P.G., Herczeg, A.L. (Eds.), Environmental Tracers in Subsurface Hydrology. Springer, pp. 175–194.
Choi, J., Harvey, J.W., Conklin, M.H., 2000. Characterizing multiple timescales of stream and storage zone interaction that affect solute fate and transport in streams. Water Resour. Res. 36 (6), 1511–1518.
Claret, C., Boulton, A., 2009. Integrating hydraulic conductivity with biogeochemical gradients and microbial activity along river–groundwater exchange zones in a subtropical stream. Hydrogeol. J. 17 (1), 151–160.
Clark, J.F., Hudson, G.B., Davisson, M.L., Woodside, G., Herndon, R., 2004. Geochemical imaging of flow near an artificial recharge facility, Orange County, CA. Ground Water 42, 167–174.
Cook, P.G., Favreau, G., Dighton, J.C., Tickell, S., 2003. Determining natural groundwater influx to a tropical river using radon, chlorofluorocarbons and ionic environmental tracers. J. Hydrol. 277 (1–2), 74–88.
Cook, P.G., Lamontagne, S., Berhane, D., Clark, J.F., 2006. Quantifying groundwater discharge to Cockburn River, southeastern Australia, using dissolved gas tracers Rn-222 and SF6. Water Resour. Res. 42 (10), W10411.
Corbett, D., Burnett, W., Cable, P., Clark, S., 1998. A multiple approach to the determination of radon fluxes from sediments. J. Radioanal. Nucl. Chem. 236 (1), 247–253.
Deforet, T. et al., 2009. Do parafluvial zones have an impact in regulating river pollution? Spatial and temporal dynamics of nutrients, carbon, and bacteria in a large gravel bar of the Doubs River (France). Hydrobiologia 623 (1), 235–250.
Deng, Z.Q., Jung, H.S., 2009. Variable residence time-based model for solute transport in streams. Water Resour. Res. 45 (3).
Dent, C.L. et al., 2007. Variability in surface-subsurface hydrologic interactions and implications for nutrient retention in an arid-land stream. J. Geophys. Res. 112, G04004.
Findlay, S., 1995. Importance of surface-subsurface exchange in stream ecosystems: the hyporheic zone. Limnol. Oceanogr. 40 (1), 159–164.
Gomez, J.D., Wilson, J.L., Cardenas, M.B., 2012. Residence time distributions in sinuosity-driven hyporheic zones and their biogeochemical effects. Water Resour. Res. 48 (9).
Gooseff, M.N., 2010. Defining hyporheic zones–advancing our conceptual and operational definitions of where stream water and groundwater meet. Geogr. Compass 4 (8), 945–955.
Gooseff, M.N., McKnight, D.M., Runkel, R.L., Vaughn, B.H., 2003. Determining long time-scale hyporheic zone flow paths in Antarctic streams. Hydrol. Process. 17 (9), 1691–1710.
Haggerty, R., Wondzell, S.M., Johnson, M.A., 2002. Power-law residence time distribution in the hyporheic zone of a 2nd-order mountain stream. Geophys. Res. Lett. 29 (13), 18-1–18-4.
Harvey, J.W., Wagner, B.J., 2000. Quantifying hydrologic interactions between streams and their subsurface hyporheic zones. In: Jones, J.B., Mulholland, P.J. (Eds.), Streams and Ground Waters. Elsevier, pp. 3–44.
Harvey, J.W., Wagner, B.J., Bencala, K.E., 1996. Evaluating the reliability of the stream tracer approach to characterize stream-subsurface water exchange. Water Resour. Res. 32 (8), 2441–2451.
Hoehn, E., Cirpka, O.A., 2006. Assessing residence times of hyporheic ground water in two alluvial flood plains of the Southern Alps using water temperature and tracers. Hydrol. Earth Syst. Sci. 10 (4), 553–563.
Hoehn, E., Von Gunten, H., 1989. Radon in groundwater: a tool to assess infiltration from surface waters to aquifers. Water Resour. Res. 25 (8), 1795–1803.
Holmes, R.M., Fisher, S.G., Grimm, N.B., 1994. Parafluvial nitrogen dynamics in a desert stream ecosystem. J. North Am. Benthol. Soc. 13 (4), 468–478.
Jackson, T.R., Haggerty, R., Apte, S.V., Coleman, A., Drost, K.J., 2012. Defining and measuring the mean residence time of lateral surface transient storage zones in small streams. Water Resour. Res. 48 (10).
Jones, J.B., Mulholland, P.J., 2000. Streams and Ground Waters. Academic Press, New York, 425 pp.
Kelleher, C. et al., 2013. Identifiability of transient storage model parameters along a mountain stream. Water Resour. Res. 49 (9), 5290–5306.
Lamontagne, S., Cook, P., 2007. Estimation of hyporheic water residence time in situ using 222 Rn disequilibrium. Limnol. Oceanogr. Methods 5, 407–416.
Lautz, L.K., Kranes, N.T., Siegel, D.I., 2010. Heat tracing of heterogeneous hyporheic exchange adjacent to in stream geomorphic features. Hydrol. Process. 24, 3074–3086.
Leaney, F., Herczeg, A., 2006. A rapid field extraction method for determination of radon-222 in natural waters by liquid scintillation counting. Limnol. Oceanogr. Methods 4, 254–259.
Lewis, D., Grimm, N., Harms, T., Schade, J., 2007. Subsystems, flowpaths, and the spatial variability of nitrogen in a fluvial ecosystem. Landscape Ecol. 22 (6), 911–924.
Marion, A., Zaramella, M., Bottacin-Busolin, A., 2008. Solute transport in rivers with multiple storage zones: the STIR model. Water Resour. Res. 44 (10).
O'Connor, B.L., Harvey, J.W., 2008. Scaling hyporheic exchange and its influence on biogeochemical reactions in aquatic ecosystems. Water Resour. Res. 44, W12423.
Payn, R., Gooseff, M., McGlynn, B., Bencala, K., Wondzell, S., 2009. Channel water balance and exchange with subsurface flow along a mountain headwater stream in Montana, United States. Water Resour. Res. 45, W11427.
Peterson, E.W., Sickbert, T.B., 2006. Stream water bypass through a meander neck, laterally extending the hyporheic zone. Hydrogeol. J. 14 (8), 1443–1451.
Ramanaidou, E., Morris, R., Horwitz, R., 2003. Channel iron deposits of the Hamersley Province, Western Australia. Aust. J. Earth Sci. 50 (5), 669–690.
Raymond, P., Cole, J., 2001. Gas exchange in rivers and estuaries: choosing a gas transfer velocity. Estuaries Coasts 24 (2), 312–317.
Runkel, R.L., 1998. One-Dimensional Transport with Inflow and Storage (OTIS): A Solute Transport Model for Streams and Rivers. US Department of the Interior, US Geological Survey.

Sawyer, A.H., Cardenas, M.B., 2009. Hyporheic flow and residence time distributions in heterogeneous cross-bedded sediment. Water Resour. Res. 45 (8).
Stonedahl, S.H., Harvey, J.W., Worman, A., Salehin, M., Packman, A.I., 2010. A multiscale model for integrating hyporheic exchange from ripples to meanders. Water Resour. Res. 46, W12539.
Storey, R.G., Howard, K.W., Williams, D.D., 2003. Factors controlling riffle-scale hyporheic exchange flows and their seasonal changes in a gaining stream: a three-dimensional groundwater flow model. Water Resour. Res. 39 (2), 1034.
Swanson, T.E., Cardenas, M.B., 2010. Diel heat transport within the hyporheic zone of a pool-riffle-pool sequence of a losing stream and evaluation of models for fluid flux estimation using heat. Limnol. Oceanogr. 55 (4), 1741–1754.
Triska, F.J., Duff, J.H., Avanzino, R.J., 1993. Patterns of hydrological exchange and nutrient transformation in the hyporheic zone of a gravel-bottom stream – examining terrestrial aquatic linkages. Freshw. Biol. 29 (2), 259–274.
Wanninkhof, R., Ledwell, J.R., Broecker, W.S., Hamilton, M., 1987. Gas exchange on Mono Lake and Crowley Lake, California. J. Geophys. Res. 92 (C13), 14567–14580.
Ward, A.S. et al., 2013. Variations in surface water-ground water interactions along a headwater mountain stream: comparisons between transient storage and water balance analyses. Water Resour. Res. 49 (6), 3359–3374.
Worman, A., Packman, A.I., Johansson, H., Jonsson, K., 2002. Effect of flow-induced exchange in hyporheic zones on longitudinal transport of solutes in streams and rivers. Water Resour. Res. 38, 1001(1).
Zarnetske, J.P., Haggerty, R., Wondzell, S.M., Baker, M.A., 2011. Dynamics of nitrate production and removal as a function of residence time in the hyporheic zone. J. Geophys. Res. Biogeosci. 116 (G1) (2005–2012).
Zarnetske, J.P., Haggerty, R., Wondzell, S.M., Bokil, V.A., González-Pinzón, R., 2012. Coupled transport and reaction kinetics control the nitrate source-sink function of hyporheic zones. Water Resour. Res. 48 (11).